



## Temperature control of continental lithosphere elastic thickness, $T_e$ vs $V_s$

R.D. Hyndman<sup>a,b,\*</sup>, C.A. Currie<sup>c</sup>, S. Mazzotti<sup>a,b</sup>, A. Frederiksen<sup>d</sup>

<sup>a</sup> Pacific Geoscience Centre, Geological Survey of Canada, 9860 W. Saanich Road, Sidney, B.C., Canada V8L4B2

<sup>b</sup> School of Earth and Ocean Sciences, University of Victoria, Victoria, B.C., Canada

<sup>c</sup> Department of Physics, University of Alberta, Edmonton, Alb, Canada

<sup>d</sup> Department of Geological Sciences, University of Manitoba, Winnipeg, Man, Canada

### ARTICLE INFO

#### Article history:

Received 21 April 2008

Received in revised form 3 November 2008

Accepted 16 November 2008

Editor: C.P. Jaupart

#### Keywords:

effective elastic thickness

$T_e$

$V_s$  tomography

lithosphere

rheology

temperature

### ABSTRACT

The elastic thickness of the continental lithosphere is closely related to its total strength and therefore to its susceptibility to tectonic deformation and earthquakes. Recently it has been questioned whether the lithosphere thickness and strength are dependent on crustal and upper mantle temperatures and compositions as predicted by laboratory data. We test this dependence regionally by comparison in northwestern North America of the effective elastic thickness  $T_e$ , from topography–gravity coherence, with upper mantle temperatures mapped by shear wave tomography velocities  $V_s$  and other temperature indicators. The  $T_e$  values are strongly bimodal as found globally, less than 20 km for the hot Cordillera backarc and over 60 km for the cold stable Craton. These  $T_e$  correspond to low  $V_s$  beneath the Cordillera and high  $V_s$  beneath the Craton. Model temperature–depth profiles are used to estimate model  $T_e$  for comparison with those observed. Only limited areas of intermediate thermal regimes, i.e., thermotectonic ages of ~300 Ma, have intermediate  $T_e$  that suggest a weak lower crust over a stronger upper mantle. There are large uncertainties in model  $T_e$  associated with composition, water content, strain rate, and decoupling stress threshold. However, with reasonable parameters, model yield stress envelopes correspond to observed  $T_e$  for thermal regimes with 800–900 °C at the Cordillera Moho and 400–500 °C for the Shield, in agreement with temperatures from  $V_s$  and other estimators. Our study supports the conclusion that lithosphere elastic thickness and strength are controlled primarily by temperature, and that laboratory-based rheology generally provides a good estimate of the deformation behaviour of the crust and upper mantle on geological time scales.

Crown Copyright © 2008 Published by Elsevier B.V. All rights reserved.

### 1. Introduction

The distribution of tectonic deformation and seismicity in the continents is controlled by the balance of plate boundary tectonic forces, internal buoyancy forces, and variations in continental lithosphere strength (e.g., Thatcher and Pollitz, 2008). The strength of the lithosphere is closely related to the temperature-controlled effective elastic lithosphere thickness ( $T_e$ ) (e.g., Burov and Diament, 1995). At shallow depths, the lithosphere deforms mainly elastically for small deformations, and through localized brittle faulting and earthquakes or shear zone motions for larger deformation. At some depth, temperatures are too high for brittle behaviour; deformation is ductile and there is a substantial reduction in strength. Because of the different compositions, the mantle may behave elastically to higher temperatures than the crust.  $T_e$  may approximately correspond to the depth of the brittle–ductile transition in the crust (as seen in deeply exposed crustal sections) for areas of very high temperatures

where there is little strength in the lower crust and upper mantle and therefore a single elastic layer. Similarly,  $T_e$  may approximate the brittle–ductile transition in the upper mantle for areas of extremely low temperatures where the entire crust and uppermost mantle are strong. For intermediate temperature regimes, the lower crust may be weak and the uppermost mantle strong, and the representation of  $T_e$  is more complex, involving the combined effect of two or more elastic layers. The effective elastic thickness  $T_e$  represents an estimate of the thickness of a simple elastic layer with equivalent elastic bending properties to those of the lithosphere (e.g., Burov and Diament, 1995).

In recent discussions, it has been questioned whether the lithosphere thickness and strength are closely related to the temperature regime, as expected from laboratory data (e.g., Jackson, 2002; Alfonso and Ranalli, 2004; Handy, 2004; Pérez-Gussinyé and Watts, 2005; Burov and Watts, 2006; Watts, 2007; Bürgmann and Dresen, 2008; Thatcher and Pollitz, 2008). A number of studies have compared the lithosphere thickness and strength to the local geotherm. Pérez-Gussinyé and Watts (2005) examined the increase in  $T_e$  with tectonic age for geological provinces in Europe and found that  $T_e$  increased substantially for ages greater than about 1000 Ma compared to younger provinces. In this study, we test the dependence of the elastic

\* Corresponding author. Pacific Geoscience Centre, Geological Survey of Canada, 9860 W. Saanich Road, Sidney, B.C., Canada V8L4B2. Tel.: +1 250 363 6428; fax: +1 250 363 6565.

E-mail address: [rhyndman@nrcan.gc.ca](mailto:rhyndman@nrcan.gc.ca) (R.D. Hyndman).

thickness on temperature regionally over a large area of western North America. We also show the large  $T_e$  for the low temperature Archean Canadian Shield compared to the high temperature Phanerozoic Canadian Cordillera.

We compare the mapped effective elastic thickness  $T_e$  from gravity–topography coherence with upper mantle temperatures mapped by shear wave velocities  $V_s$  from seismic tomography and other temperature constraints. Model temperature–depth profiles, combined with laboratory rheology data, allow us to estimate model  $T_e$  for different regions. The  $V_s$ -based temperatures are at a fixed mantle depth whereas  $T_e$  is controlled by mid-crustal temperatures for the hot Cordillera and by upper mantle temperatures for the cold Craton. We therefore have not attempted to calculate  $T_e$  from  $V_s$  directly; we have used temperatures from a simple lithosphere cooling model that correspond well at early times to the estimates of Cordillera temperature–depth, and to Craton temperature–depth estimates for later times. In the upper mantle, velocity is controlled primarily by temperature with compositional variations usually being only a second order effect (e.g., Goes et al., 2000; Wiens and Smith, 2003; Cammarano et al., 2003). The main composition effect is the small difference in the upper mantle  $V_s$  versus temperature relation for the young chemically fertile Cordillera compared to the more depleted Craton and stable platform (e.g., Griffin et al., 2003).

We include in the “Craton” designation the Slave, Wopmay, Canadian Shield, Western Canada Sedimentary Basin, and Interior Platform, of Paleozoic and older basement ages. The thermally-defined Cordillera–Craton boundary is just west of the mountain front, approximately at the Rocky Mountain Trench in southern British Columbia (see Fig. 2 for location) as indicated by heat flow data and crustal thickness (e.g., Hyndman and Lewis, 1999). A variety of other data indicate that this is the edge of the strong cold Craton lithosphere, including the eastern limit of Tertiary volcanism, short wavelength to long wavelength transition in magnetic anomalies, and volcanic xenoliths (e.g., Gabrielse and Yorath, 1991). The boundary approximately follows the Tintina Fault to the north. The Volcanic Arc zone was defined by an approximately 100 km wide band centered on the volcanic centres. This is approximately the spatial resolution of our data.

We focus mainly on the region of northwestern North America between latitudes 48° and 64°N, to avoid areas of current strong deformation where rapid lateral variations in strain rates and other processes add complexity: i.e., Basin and Range extension, Yellowstone hot spot, Columbia Plateau young volcanic terrane, current deformation in the Yukon–Alaska region, and the Cascadia forearc where the downgoing oceanic plate is expected to give anomalous velocities and  $T_e$ . We discuss the anomalous  $T_e$  for these areas briefly below. In our main study area, the last major regional deformation was foreland belt thrust shortening in the late Cretaceous–early Tertiary (e.g., Gabrielse and Yorath, 1991). There was significant Eocene extension in a restricted area of southeastern British Columbia, and early to mid-Tertiary strike-slip faulting through central British Columbia (e.g., Gabrielse and Yorath, 1991). There was subduction along the whole margin prior to about 50 Ma that was then cut off by transform faulting on the Queen Charlotte margin (e.g., Engebretson et al., 1984). Subduction has continued on the Cascadia margin south of about 50°N.

## 2. Effective elastic thickness, $T_e$ , from gravity–topography coherence

### 2.1. Computation of $T_e$

The effective elastic thickness of the continental lithosphere,  $T_e$  (e.g., Burov and Diament, 1995; Watts and Burov, 2003), provides an important tool for regional mapping of the thickness and strength of the lithosphere and its susceptibility to tectonic deformation.  $T_e$  is determined from the wavelengths over which the topography and

gravity (a measure of internal mass distribution and lithosphere flexure) are well correlated (e.g., Burov and Diament, 1995).  $T_e$  is related to the flexural rigidity and the characteristic bending wavelength of the lithosphere (e.g., Macario et al., 1995).  $T_e$  may be estimated reliably in a few local areas through forward modelling of the deformation due to local loads but regional mapping requires spectral methods using the coherence (or admittance) between topography and gravity. This method has been used extensively to map  $T_e$  in many areas globally. There has been debate on admittance versus coherence methods for calculating  $T_e$ , but an important recent conclusion is that the Bouguer gravity coherence method and free-air gravity admittance method yield comparable  $T_e$  results when consistently formulated (Pérez-Gussinyé and Watts, 2005). For areas with a single elastic layer, i.e., very hot or very cold lithosphere,  $T_e$  may be expected to approximate the depth of the brittle–ductile transition (downward transition from narrow fault zones to broad shear zones).

There are high-quality gridded gravity and topography data with consistent spatial resolution over our whole study area. The  $T_e$  data for our analysis comes from Flück et al. (2003) for western Canada and from Lowry et al. (2000) for western United States. Wang and Mareschal (1999) found very similar results to these two studies for an overlapping region of the Canadian Shield (see these three articles for references to earlier work in the region). Generally similar results also have been obtained by Audet et al. (2007) for western Canada and by Poudjom Djomani et al. (2005) for the Slave Province, although the latter authors found the northern part of the Craton is characterized by a relatively weak lithosphere.

The  $T_e$  data used the maximum entropy-based spectral estimator as described by Lowry and Smith (1994) that reduces the data horizontal spatial windows and therefore gives higher spatial resolution than previous methods. Different analysis window sizes are needed for the different areas, smaller for the Cordillera where the lithosphere is thin and larger for the Craton where the lithosphere is thick (e.g., Flück et al., 2003). It is important to note that the maximum  $T_e$  thickness that can be reliably resolved depends on the horizontal window size used (e.g., Swain and Kirby, 2003; Pérez-Gussinyé et al., 2004). For the Craton, Flück et al. (2003) used 800×800 km so the  $T_e$  values over about 85 km are not accurately determined and there may be a bias to estimates that are too low. The spatial resolution of  $T_e$  is 10's of km where the lithosphere is thin and the horizontal bending wavelengths are short, especially within the Cordillera, but 100's of km where the lithosphere is thick and bending horizontal wavelengths are long, especially for the Craton.

There are a number of questions and uncertainties with this spectral method (e.g., discussions by Pérez-Gussinyé and Watts, 2005, 2007; Lowry and Smith, 1994). In addition to the computational methods used, the ages and durations of the loads that produce the lithosphere flexure may be substantially different for different regions, especially young tectonically active areas compared to older stable areas. This may be important because of the strain rate dependence of crustal and mantle rheology (e.g., Kohlstedt et al., 1995). The analysis method takes into account that there is surface and internal loading but difference in the form of the loads may still be important. For example, there is significant loading by topography for the Cordillera mountain belt, whereas the loads can be due to internal crustal density variations for the Craton (e.g., Forsyth, 1985). Also, the normal loads in cratons are generally smaller than in young areas, so that the flexural response is smaller and not as well resolved. We have ignored  $T_e$  anisotropy as examined by Audet and Mareschal (2004) and Audet et al. (2007) assuming that it is approximately azimuthally averaged. Because of these complexities, caution is required for detailed quantitative interpretation of the  $T_e$  data. However, the mapped variations in loading flexural wavelength are large, so  $T_e$  results of sufficient accuracy can be obtained to allow important conclusions.

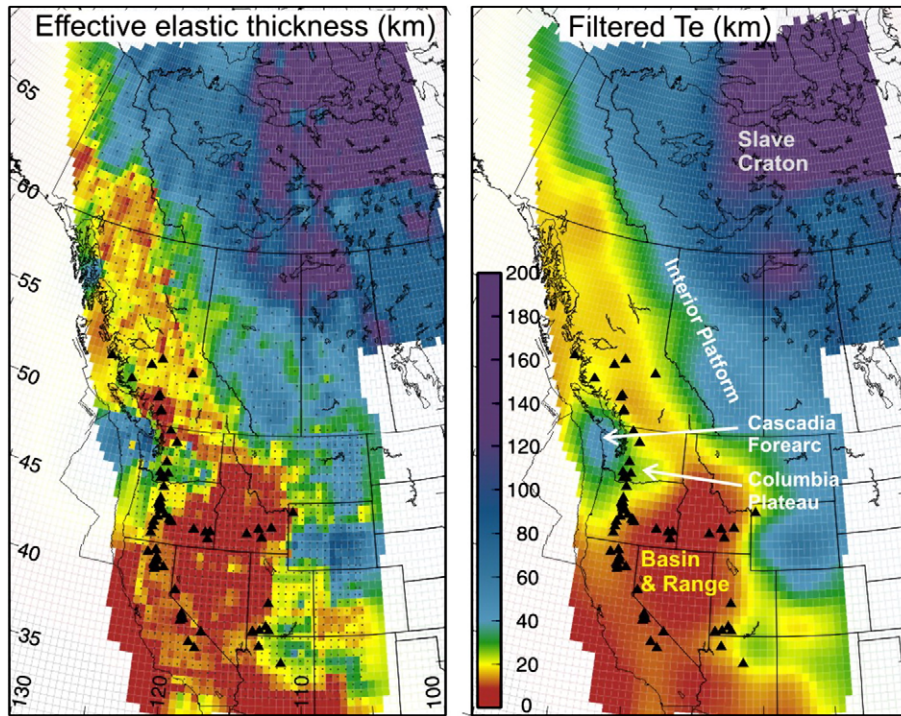


**Fig. 1.** Effective elastic thickness,  $T_e$ , for Canada–U.S. Cordillera and adjacent Craton. Left: unfiltered data. Right: spatially smoothed data with a Gaussian weighting function diameter 600 km, to match resolution of  $V_s$  data. Most of Cordillera has  $T_e < 20$  km; most of Craton has  $T_e > 60$  km.

2.2.  $T_e$  results

The  $T_e$  distribution for the Canadian and USA portions of western North America is shown in Fig. 1, both unsmoothed and spatially smoothed using a Gaussian weighting function with diameter 600 km. This is comparable to the smoothing used in the  $V_s$  tomography data. The unsmoothed data contain more spatial detail but much of that detail may be data noise or uncertainty. There is a clear bimodal distribution with values generally less than 20 km for the Cordillera (present or recent backarc), i.e., elastic strength is limited to the upper crust, and thick  $T_e > 60$  km, over most of the Craton region to the east, i.e., all of crust and a substantial thickness of upper mantle (Figs. 1 and 2). The thin  $T_e$  values are well correlated with the generally high topography and

high heat flow of the Cordillera (e.g., Hyndman et al., 2005). Fig. 2 illustrates the clear regional correlation between  $T_e$  and upper mantle  $V_s$  for the northern Cordillera and adjacent Craton. Thin  $T_e$  corresponds to slow  $V_s$  (and high inferred temperatures) and thick  $T_e$  to fast  $V_s$ . Below, we examine quantitatively the relation between the two parameters and their control by temperature.

There is a comparable bimodal distribution between the Cordillera and Craton of South America (Pérez-Gussinyé et al., 2007), and global studies have found that the distribution of  $T_e$  is similarly bimodal, i.e., 10–30 km and 70–90 km (Watts, 1992). This bimodal distribution is consistent with the conclusion that current or recent backarc mobile belts such as the Cordillera have similar thin hot lithospheres (Hyndman et al., 2005; Currie and Hyndman, 2006) and cratons and

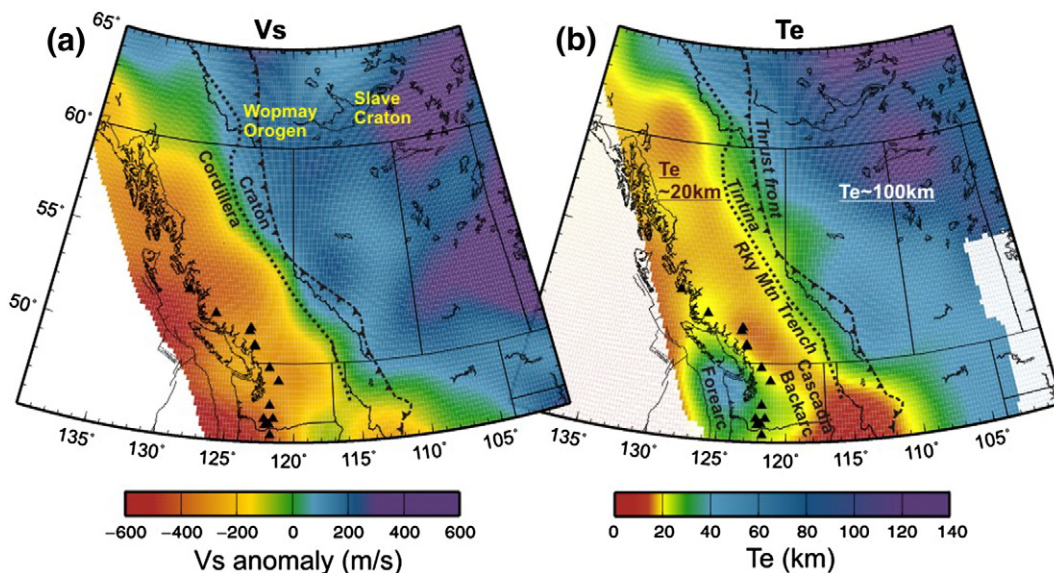


**Fig. 2.** Tomography shear-wave velocities,  $V_s$ , at 100 km compared with the effective elastic thickness,  $T_e$ , for the northern Cordillera and adjacent Craton.

other tectonically old areas are consistently cold. Backarc lithosphere temperatures appear to decay with a thermal time constant of about 300 Ma following termination of subduction (e.g., Currie and Hyndman, 2006). Only intermediate thermo-tectonic age regions, i.e., ~300 Ma, such as the Appalachians of eastern North America (e.g., Audet and Mareschal, 2004), and areas in Europe (e.g., Pérez-Gussinyé and Watts, 2005) show large areas of intermediate  $T_e$  (50–60 km) that suggest a layered rheology with a weak zone in the lower crust over a strong uppermost mantle.

### 2.3. $T_e$ in special areas

There are several local regions of anomalous  $T_e$  in western North America that we do not address in our main analysis (Fig. 1):

- (1) The coastal region from Vancouver Island to N. California has a  $T_e$  of about 50 km. This region is in the current forearc of the Cascadia subduction zone and likely has a higher  $T_e$  than the rest of the Cordillera due mainly to the low forearc temperatures. Although probably decoupled from the overlying forearc by the subduction thrust, the underthrusting oceanic lithosphere may also add to the effective elastic thickness. The thick  $T_e$  for the Cascadia subduction zone forearc probably extends to northernmost California, but only limited  $T_e$  data are available there. Compared to the remainder of the Cordillera,  $T_e$  may be larger in the Alaska Panhandle which is interpreted to be a former (~40 Ma) cool forearc, but there is little data available for this area. The Queen Charlotte region also is a former forearc but it had mid-Tertiary extension that may have heated and thinned the lithosphere.
- (2) The Basin and Range area of the central U.S. Cordillera exhibits unusually small  $T_e$  values of less than 10 km (Lowry and Smith, 1995), probably associated with weakening by the ongoing extensional faulting such that the lithosphere does not behave elastically (e.g., Hassani and Chéry, 1996). High crustal temperatures produced by current extension also undoubtedly play a role.
- (3) The Columbia Plateau Miocene volcanic area of south central Washington State exhibits thicker  $T_e$  than the average for the Cordillera. This is an unexplained anomaly in the Cordillera that warrants further investigation. The thick  $T_e$  may be due to lower temperatures as suggested by the  $V_s$  data or to an especially mafic crustal composition that is stronger at the same temperature compared to average composition continental crust.

### 3. Shear wave tomography

There are many constraints to lithosphere temperatures in local areas, including heat flow-heat generation measurements, mantle xenoliths,  $P_n$  uppermost mantle velocities, and thickness of the lithosphere (e.g., Currie and Hyndman, 2006). However, upper mantle seismic velocities appear to be the best thermal constraint that can be mapped consistently over large areas (e.g., Goes and van der Lee, 2002). In this study, we use  $V_s$  to determine regional lithosphere temperatures and include other temperature indicators to confirm the temperatures from  $V_s$ . As discussed below, temperature is the dominant control of upper mantle seismic velocity (e.g., Goes et al., 2000; Wiens and Smith, 2003), in contrast to the crust where composition is usually the main control. Previously, we compared temperatures from  $V_s$  of subduction backarcs globally with those from the main other temperature constraints for the deep crust and upper mantle and found general agreement (Hyndman et al., 2005; Currie and Hyndman, 2006).

We follow Goes and van der Lee (2002) and use shear wave velocity  $V_s$  from surface wave tomography. One limitation of the  $V_s$  data is the quite low vertical resolution, 25–50 km, and low horizontal resolution, 100–200 km. There are  $V_s$  estimates for the whole region, but for the northernmost part there are fewer seismograph stations

and fewer rays through the region so there is lower accuracy and poorer spatial resolution (see below). We have used the western North America  $V_s$  data from the recent model NA-04 by van der Lee and Frederiksen (2005), a combined and updated solution following earlier more regional studies (van der Lee and Nolet, 1997; Frederiksen et al., 2001). We use tomography data from 60 to 200 km depth to calculate temperatures. The data allow us to estimate temperature-depth profiles for comparison with other temperature indicators to check the validity of the  $V_s$  temperatures. In a few areas, there are anomalous  $V_s$  values inconsistent with other temperature constraints. These values are mainly in the northernmost region and some areas along the coast where the data coverage is poor. We therefore have restricted our analysis to the higher quality  $V_s$  data using a measure of coverage density (Fig. 3) from van der Lee and Frederiksen (2005) to retain about 50% of the best constrained data within the main study area covered by  $T_e$  data. The coverage density measurement used is the sum of all sensitivities for each grid cell, i.e., the sum of each column of the tomographic matrix. Using only the better-constrained data (shaded area of Fig. 3) reduced the scatter in the  $T_e$  vs  $T$  plots shown below by about a factor of two, and removed many of the anomalous inferred temperatures.

Temperatures at a depth of 100 km are used for our main regional analysis and comparison with  $T_e$  observations. Using temperatures at 100 km and deeper for calculation of model  $T_e$  has the problem of nearly constant temperatures (adiabatic) within the convecting asthenosphere. The base of the Cordillera thermal lithosphere is about 60 km based on other data (e.g., Hyndman et al., 2005 and references therein; Currie and Hyndman, 2006; Harder and Russell, 2006), so there is only a small difference between temperatures (and  $V_s$ ) at 60 km compared to those at 100 km and deeper for the Cordillera. For thin lithospheres ( $T_e < 60$  km), changes in  $T_e$  will be associated with only small variations of  $V_s$  at 60 km and deeper.

The map of  $V_s$  at 100 km compared to  $T_e$  (Fig. 2) shows clear qualitative agreement. The boundary between high and low  $V_s$  is similar to that for  $T_e$ , i.e., approximately the Rocky Mountain Trench and the Tintina Fault to the north, in agreement with this being the main thermal boundary (e.g., Hyndman and Lewis, 1999).

### 4. Conversion of $V_s$ to temperature

Temperature is the primary control of  $V_s$  for the upper mantle (e.g., Goes et al., 2000; Wiens and Smith, 2003; Cammarano et al., 2003). The main second order effects are variations in composition, anisotropy, water content, and partial melt. We deal with the regional

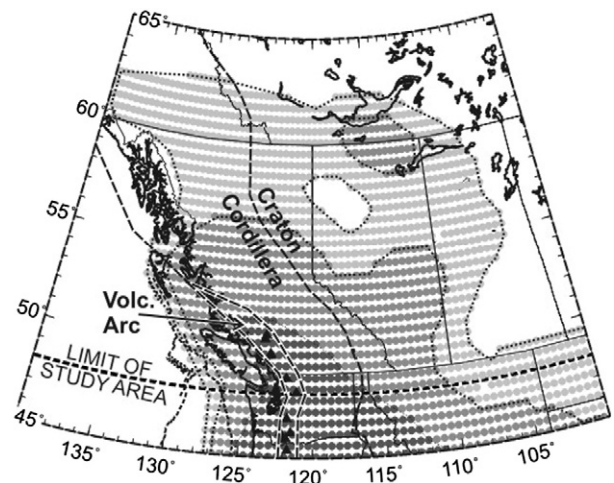


Fig. 3.  $V_s$  data quality map for western Canada based on coverage density values. Blank: no  $T_e$  data in primary source or poor  $V_s$  quality. Light grey: data quality in the top 50%. Medium grey: top 33%. Dark grey: top 15%. The data regions for the three temperature-depth profiles of Fig. 6 are shown.

composition difference between the more refractory compositions of older cratonic regions compared to younger, more fertile mantle compositions in tectonically active areas (see below and Supplementary Material, Appendix A). The effects of anisotropy are reasonably averaged by the variable propagation directions in the tomography data. The presence of water or partial melt will cause a reduction in seismic velocities, but the relationship between water and melt content and velocity is poorly constrained (e.g., Goes et al., 2000; Wiens and Smith, 2003) and we do not include these factors in the temperature estimates from  $V_s$ . Laboratory data suggest that the presence of water primarily reduces seismic velocities by enhancing anelasticity (e.g., Karato, 2003), and thus neglecting the effects of water could lead to an overestimation of the temperatures in the hotter areas (e.g., Cordillera) where anelasticity is significant (temperatures  $>1000$  °C). Because we use a strongly temperature-dependent anelasticity factor in the calculations (Supplementary Material, Appendix A), we estimate that the calculated temperatures could be  $\sim 50$  °C too high if the Cordillera upper mantle is substantially hydrated. It may be possible to examine the effect of water content by comparison of the temperatures estimated from  $V_p$  and from  $V_s$  data (e.g., Goes and van der Lee, 2002; Dixon et al., 2004), but there are only limited  $V_p$  tomography data for our main study area to examine this effect. Laboratory measurements and theoretical models suggest that the velocity reduction due to partial melt becomes significant for melt fractions greater than 1–2% (Wiens and Smith, 2003). Therefore we expect that partial melt is important only for a few regions where there may be a significant melt fraction, such as the Cascadia Volcanic Arc (see Fig. 6) and the Basin and Range (e.g., Dixon et al., 2004).

For conversion of  $V_s$  to temperature we use laboratory-based mineral elastic properties as a function of temperature, pressure, and composition (Supplementary Material, Appendix A). The resulting velocity-temperature relationship is then used to calculate the 3-dimensional upper mantle temperature distribution to a depth of 200 km. Fig. 4 shows the temperature  $T$  versus  $V_s$  relationship based on the Tecton, Proton, and Archon composition models of Griffin et al. (2003). At high temperatures, all compositions have similar  $V_s$ - $T$  relationships, but below 500 °C, the Archon composition yields temperatures  $\sim 200$  °C higher, due to the effect of chemical depletion. The temperature uncertainty due to the  $V_s$  versus  $T$  relation is 50–100 °C for a reasonable range of parameters (Supplementary Material, Appendix A).

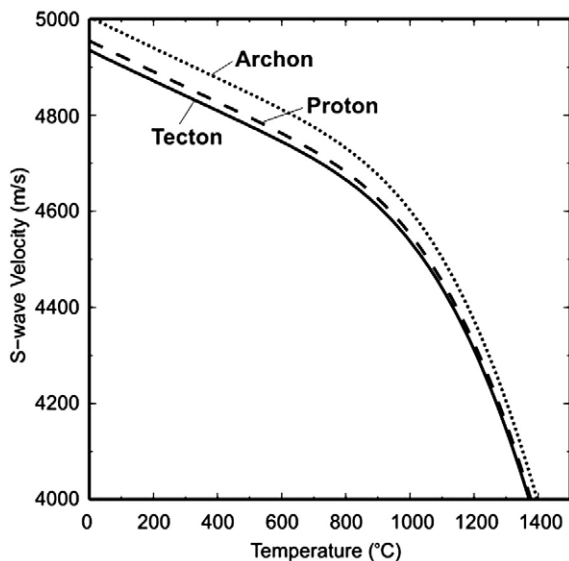


Fig. 4. Relation between S-wave velocity,  $V_s$ , and temperature for several compositions; "Tecton" for Cordillera, and "Archon" and "Proton" for Craton.

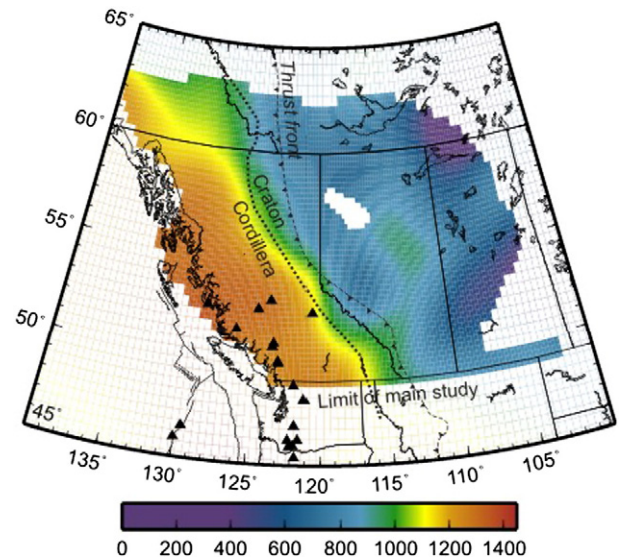


Fig. 5. Temperature (°C) at 100 km depth from  $V_s$  tomography in main analysis area. The Cordillera temperatures use the Tecton  $V_s$ - $T$  relation and the Craton temperatures use the Proton relation.

We use the Tecton composition for the Cordillera and the Proton composition for the stable Craton, where the mantle xenolith data suggest a more depleted mantle lithosphere (e.g., Griffin et al., 2004). The Archon relation gives Craton temperatures that are about 50 °C higher than inferred from xenolith thermobarometry data. Calibration of the  $V_s$ - $T$  relationships is provided by other temperature constraints, especially Craton xenoliths (e.g., MacKenzie and Canil, 1999 and references therein for Slave Craton), and Moho temperatures and lithosphere thicknesses for the northern Cordillera (e.g., Clowes et al., 1995; Hyndman et al., 2005; Currie and Hyndman, 2006; Harder and Russell, 2006). They indicate that the  $V_s$  temperatures are accurate to about 100 °C at 100 km depth for most areas ( $V_s$  uncertainty, plus  $V_s$  versus  $T$  relation uncertainty). Fig. 5 shows a map of the calculated temperatures at 100 km for our study area. A heat flow map could be produced from the  $V_s$  data but, first this would require assumptions for crustal heat generation, and second there should be little variation in heat flow with  $V_s$  for lithosphere thinner than 60 km since the deeper temperatures should be adiabatic.

## 5. Temperature versus depth from $V_s$ data

The  $V_s$  data allow us to estimate temperature versus depth for the Cordillera, Volcanic Arc and Craton (Fig. 6). The figure provides histograms of frequency of occurrence of temperatures in the  $V_s$  grid for the whole study region at 20 km depth increments from 60 to 200 km and the average temperatures with depth and the standard deviations at each depth for the three regions. Our Cordillera temperatures are about 50 °C lower than those of Goes and van der Lee (2002) because we use a more strongly temperature-dependent anelasticity correction (Supplementary Material, Appendix A).

In Fig. 6b, our results for the three regions are compared to the temperature versus depth from other constraints, including thermal models constrained by heat flow and heat generation data, and xenoliths (summarized by Currie and Hyndman, 2006). The Cordillera temperatures from  $V_s$  are in excellent agreement with the other estimators. The thermal lithosphere is approximately 60 km thick. Deeper temperatures increase slowly, close to the expected mantle asthenosphere adiabat maintained by convection at temperatures just below first melting (solidus). These uppermost mantle temperatures are consistent with Moho temperatures of about 900 °C from heat flow — heat generation models,  $P_n$  velocities, and upper mantle xenoliths (Fig. 6).

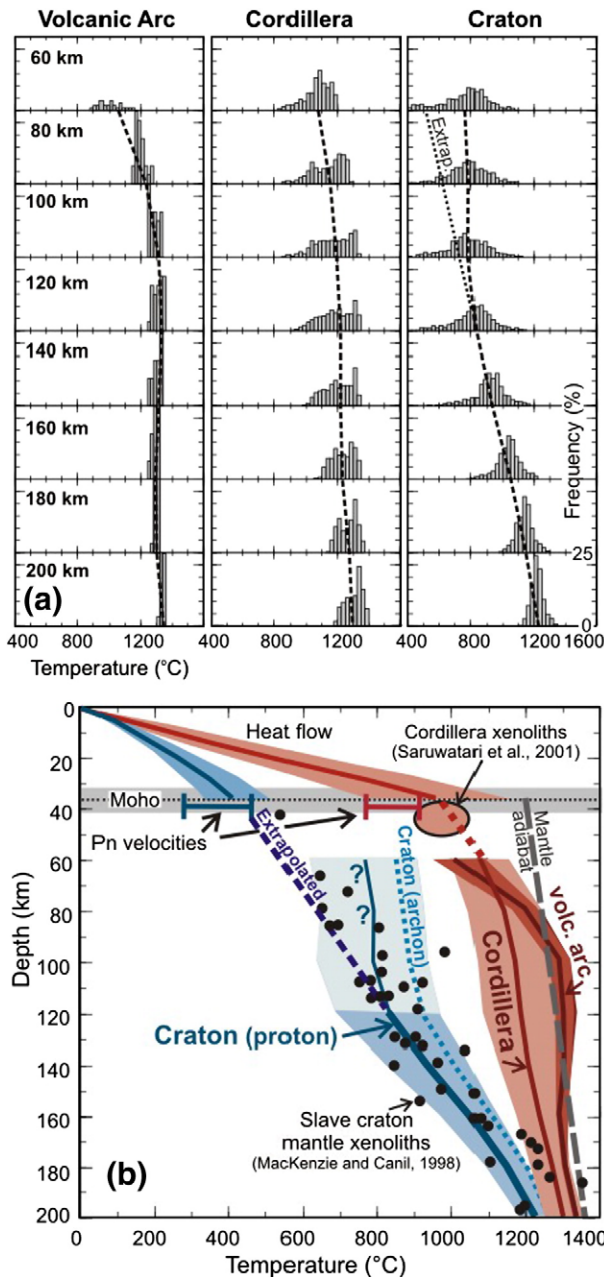


Fig. 6. (a) Frequency of occurrence temperature histograms. The dashed lines join mean temperatures at each depth. (b) Temperature–depth from Vs for Volcanic Arc, Cordillera and Craton compared to several other temperature constraints. The “extrapolated” Craton line is close to the xenolith and crustal  $T$ – $Z$  estimates.

For the Cascadia Volcanic Arc at 60 km and deeper than 180 km, the temperatures are similar to the Cordillera average, but the Volcanic Arc has higher inferred temperatures between 80 and 160 km depths that may be associated with unusually high temperatures and with partial melt beneath the arc. Local high water content also may be important. We have averaged the Vs data from a broad 100 km wide zone along the arc (Fig. 3), and more immediately beneath the volcanic zone the temperatures or melt fraction may be higher than this average. Low Vs beneath volcanic arcs interpreted to be due to rising water-rich melts observed elsewhere (e.g., Wiens and Smith, 2003), for example for Japan (Nakajima et al., 2001), and South America (Koulakov et al., 2006).

For the Craton and stable platform, there are consistent inferred temperatures that are in good agreement with those from mantle

xenoliths in the region (e.g., MacKenzie and Canil, 1999, and references therein) and for other cratons, i.e., base of thermal lithosphere at 200–250 km. Even after selecting for the higher quality Vs data, there still are systematically low Vs and high calculated temperatures at 60–80 km depth for the Craton that are inconsistent with the deeper Vs data and with other temperature constraints. Systematically low Vs and inferred high temperatures were also evident in the data of Goes and van der Lee (2002), although not as pronounced. These high calculated temperatures cannot be explained with a reasonable range of velocity–temperature relations for different mantle compositions (see Supplementary Material, Appendix A). The slow Vs (and high inferred temperatures) may be due to the vertical smoothing of velocities such that the calculated uppermost mantle Vs is reduced through the effect of the low-velocity overlying crust that has not been represented with adequate accuracy. An alternative possibility is that the uppermost mantle lies above the Hales discontinuity (Hales, 1969) which marks the spinel–garnet transition, as proposed by Lebedev et al. (2008). In the shallow spinel stability field, the velocity may be lower, resulting in higher apparent temperatures.

The upward extrapolation of temperatures deeper than 100 km yields good agreement with the Moho temperatures of about 400 °C from heat flow – heat generation models and Pn velocities (Fig. 6).

## 6. Relation between $T_e$ and upper mantle temperature

We now examine the regional relationship between  $T_e$  and Vs, and between  $T_e$  and temperature based on Vs. Fig. 7 shows the effective elastic thickness  $T_e$  versus both observed Vs and the calculated temperatures at 100 km. The scatter of derived temperatures appears much larger than that for Vs because of the non-linear relation between Vs and calculated temperature. The Cordillera values are generally separated from the Craton values, with limited overlap. The Volcanic Arc points have a similar range of  $T_e$  to the Cordillera but extend to slightly lower velocities and higher inferred temperatures. There are a number of anomalous Craton points with small  $T_e$  and low temperatures at 100 km. Many but not all are from the Western Canada Sedimentary Basin where the thick sediment section with significant radioactive heat generation and low thermal conductivity give a high temperature gradient in the upper section (including sediments) and therefore a thin  $T_e$ , but affect the deep temperature gradient (and Vs at 100 km) much less.

Although the data are scattered, there is a clear pattern of a rapid decrease in  $T_e$  at velocities below about 4700 m/s and 100 km temperatures above about 900 °C. The Cordillera backarc has thin  $T_e$  everywhere, on average ~18 km (excluding the cold thick forearc coastal area), and high temperatures at 100 km. There are very constant  $T_e$  values of ~18 km for the Volcanic Arc, similar to the Cordillera. However, the 100 km velocities are significantly lower and computed temperatures higher than for the remainder of the Cordillera. The lack of correlation between  $T_e$  and Vs suggests that these low Vs values may be due to the effect of upper mantle water or partial melt rather than high temperatures. Our relation between  $T_e$  and Vs is comparable to that of Pérez-Gussinyé et al. (2007) for South America, where there is a nearly constant  $T_e$  for a range of slow Vs at 100 km as expected for adiabatic temperatures where the lithosphere is less than 100 km thick (discussed below). This variable Vs anomaly at ~100 km (with nearly constant  $T_e$ , and inferred shallow temperatures) has the potential for productive further study using global  $T_e$  and Vs data for volcanic arcs.

The Craton generally has thick  $T_e$  (i.e., crust and significant thickness of the upper mantle) and low temperatures at 100 km. We have subdivided the stable areas further to examine the relation of  $T_e$  and Vs for the different stable geological provinces. The Interior Platform (Western Canada Sedimentary Basin) (location in Fig. 1) has a somewhat thinner  $T_e$  average of ~60 km and the lowest Vs compared to the other

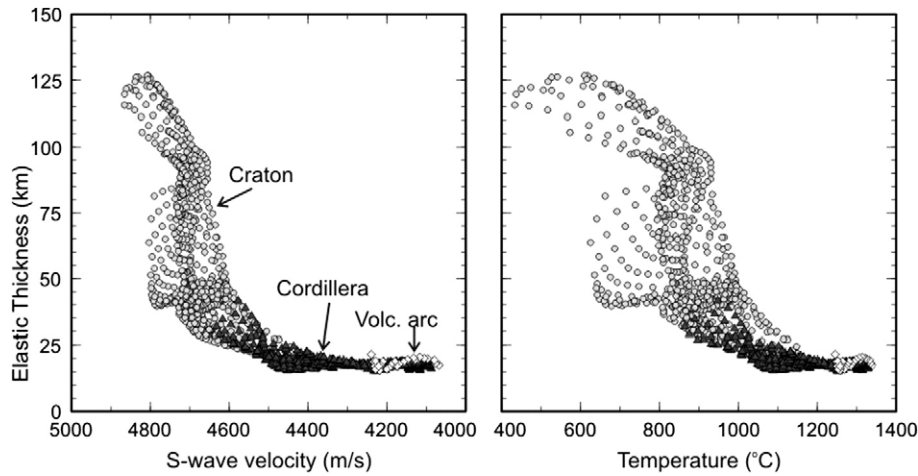


Fig. 7. Left: Elastic thickness,  $T_e$ , versus  $V_s$ . Right:  $T_e$  versus inferred temperatures. Open diamonds – Volcanic arc; Solid triangles – Cordillera, Grey circles – Craton.

stable areas, probably reflecting, (a) the higher lithosphere temperatures due to the thick layer of insulating sediments in the Interior Platform, (b) higher than average radioactive heat generation in the thick sediments, contributing to higher temperatures, and (c) for  $T_e$ , that the sediments may be weak. The other stable provinces have very similar  $T_e$  averages of  $120 \pm 21$  km, and temperatures at  $100$  km of  $852 \pm 92$  °C, with no statistically significant differences.

## 7. Model $T_e$ as a function of thermal regime and age

In this section we calculate the effective elastic thicknesses as a function of the thermal regime, using estimates of appropriate composition, strain rates, and mechanical decoupling threshold parameters in a simple analytical model. A more precise analysis would require numerical modeling. The critical controlling parameters are sufficiently uncertain that an approximate analytical method appears adequate. We present a summary of our method here. Further details are given in the Supplementary Material, Appendix B.

To simplify the range of temperature–depth profiles with geological age, we use the simple cooling model of Currie and Hyndman (2006). This model assumes conductive cooling as a function of time from an initial temperature–depth profile appropriate for a hot backarc mountain belt and in agreement with our Cordillera temperatures based on  $V_s$ . It is assumed that shallow asthenosphere convection stops quickly after termination of subduction and that this termination time approximates the commonly identified “thermotectonic age”, i.e., the time since the last major igneous, metamorphic, and deformation events. The initial profile has temperatures at the Moho of about 850 °C and below about 60 km depth has slowly increasing temperatures of 1100–1400 °C that approximate the adiabatic gradient. The cooling time constant is about 300 Ma. At times >600 Ma, the Moho temperature is 400–500 °C.

For each temperature–depth profile, we calculate the differential stress profile (e.g. Fig. 8) based on a combination of elastic bending stress, brittle yield stress, and viscous creep stress (e.g., Kohlstedt et al., 1995; Ranalli, 1995; Lowry et al., 2000). The brittle behaviour follows Coulomb’s friction criterion for pre-existing faults at failure equilibrium and assumes a dominant reverse fault mechanism (cf. Supplementary Material, Appendix B). In the ductile regime, we use a power-law rheology for dislocation creep (e.g., Ranalli, 1995) and glide controlled deformation where appropriate. We discuss these relationships and the stress threshold that defines the bottom of the elastic layers in the Supplementary Material, Appendix B.

We calculate  $T_e$  using the leaf-spring approximation (e.g., Burrov and Diament, 1995) consisting of the cubic sum of individual (decoupled) layer thicknesses. As shown in Appendix B, this approximation is valid

under the typical range of plate curvature ( $10^{-9}$ – $10^{-8}$  m $^{-1}$ ) and elastic thickness (20–100 km) of our study area. Under these conditions, the leaf-spring approximation is equivalent to the more complete “summation of the bending moment” method (e.g., Burrov and Diament, 1995; Lowry et al., 2000). The critical factor of this approximation is that the elastic fiber stress be smaller than the yield stress (brittle or creep), which corresponds to a material deforming elastically rather than plastically, i.e., for stronger curvatures, the lithosphere would yield plastically and not bend elastically. This condition is met by using a “decoupling stress threshold” of ~10 MPa (cf. Appendix B).

The cooling model temperature–depth profiles and laboratory rheologies applicable to the Cordillera and Craton are used to calculate differential stress profiles as a function of depth, i.e., “strength envelopes”, for different thermotectonic times (Fig. 8). The ductile rheologies include typical “wet” and “dry” compositions for the upper, middle, and lower crust and the mantle lithosphere (Table B1). For each thermotectonic age, we calculate stress profiles for two end-member cases: a weak lithosphere (using wet rheologies) and a strong lithosphere (using dry rheologies). We vary the strain rates from  $10^{-15}$  s $^{-1}$  to  $10^{-21}$  s $^{-1}$  to capture the range of possible deformation rates from active tectonic/plate boundary regions to stable intraplate regions. The main sources of uncertainties in the stress profiles and  $T_e$  calculations are (1) the

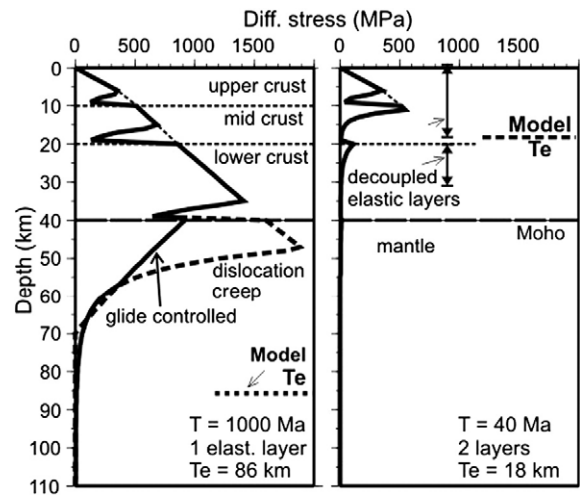
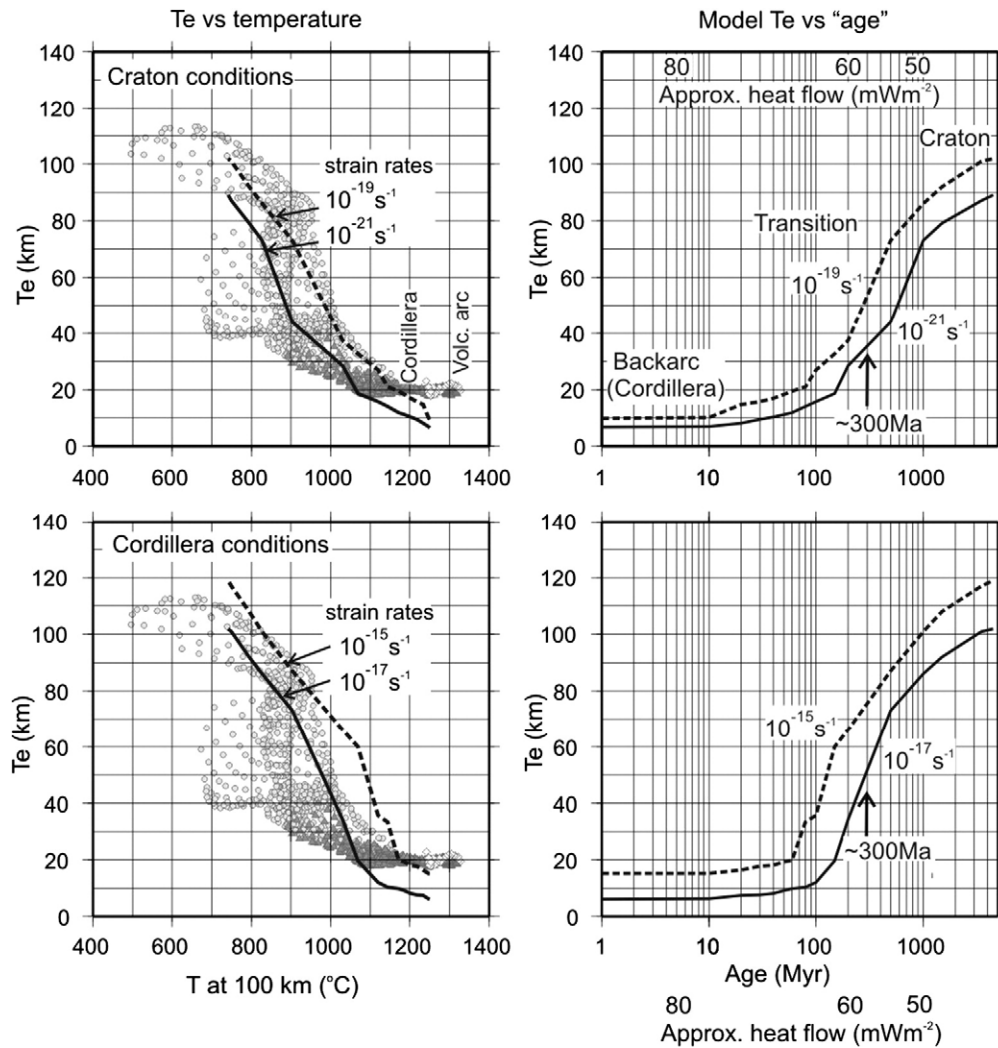


Fig. 8. Calculated strength versus depth for a model for the Craton ( $10^{-19}$  s $^{-1}$  strain rate) (left) and for the Cordillera ( $10^{-15}$  s $^{-1}$  strain rate) (right). The weak crustal layers depend on the details of the crustal compositions assumed; in these examples they do not produce decoupling so do not significantly affect the elastic thicknesses. These models give  $T_e$  in general agreement with those measured.



**Fig. 9.** (Left)  $T_e$  versus temperature from Vs, compared to model predictions using rheologies and strain rates appropriate for Cordillera and Craton. (Right) Model  $T_e$  versus thermotectonic age using temperatures from the simple model for backarc cooling by Currie and Hyndman (2006) following termination of subduction. There is a rapid increase in model  $T_e$  at about 300 Ma. Approximate heat flows are also shown.

rheology used for each layer (mafic versus felsic, dry versus wet), (2) the strain rate, which is assumed to be uniform with depth, and (3) the decoupling stress threshold.

Fig. 9 shows calculated  $T_e$  as a function of temperature at 100 km depth for the wet (Cordillera) and dry (Craton) lithosphere models and several example strain rates. There is a somewhat better fit of the Cordillera models to the Cordillera data and Craton models to the Craton data. There is some flattening of the model  $T_e$  values at Vs temperatures above about 1100  $^{\circ}\text{C}$  but not as pronounced as in the data. At these high Vs temperatures, most models predict  $T_e$  thinner than observed, suggesting that the very low velocities are at least in part produced by the effect of volatiles rather than especially high temperatures. As noted for the Volcanic Arc data, this misfit suggests that the calculated temperatures above about 1100  $^{\circ}\text{C}$  are biased too high due to the effect of upper mantle water and partial melt.

If we assume that the wet lithosphere model is representative of the Cordillera rheology, Fig. 9 shows that a fast strain rate of  $10^{-15} \text{ s}^{-1}$  is required to match the  $T_e$  data in the Cordillera ( $T_e \approx 20 \text{ km}$ ), in good agreement with estimated strain rates for active tectonics plate boundary regions (e.g., Zoback et al., 2002). Lower strain rates result in a thinner (weaker) elastic lithosphere that significantly under-predicts the measured  $T_e$ . For colder geotherms, the wet and fast strain rate lithosphere model significantly over-predicts the Craton  $T_e$  data. Fig. 9 shows the calculated  $T_e$  for a dry (strong) lithosphere

model representative of Craton rheology. For this model, slow strain rates of  $10^{-19}$  to  $10^{-21} \text{ s}^{-1}$  give reasonable fits to the data, in agreement with estimated intraplate strain rates based on seismicity and long-term deformation rate proxies (e.g. Mazzotti and Adams, 2005). However, as noted earlier, the observed  $T_e$  for the Craton may be biased too low because of finite analysis spatial window used.

Fig. 10 shows the effect of lower crustal composition on the  $T_e$  versus 100 km temperature relation. The laboratory data for quite weak compositions (e.g., felsic granulite) give substantially lower  $T_e$  in the temperature range from 900 to 1200  $^{\circ}\text{C}$  and a better fit to the data compared to the more mafic compositions. There is little effect at lower temperatures at which the upper mantle strength dominates.

We have calculated model  $T_e$  as a function of thermotectonic age using the cooling backarc model of Currie and Hyndman (2006) with their average crustal heat generation ( $1.3 \mu\text{Wm}^{-3}$  for upper 10 km and  $0.4 \mu\text{Wm}^{-3}$  for the lower 25 km of the crust) (Fig. 9). This model is similar to the constant thickness ocean lithosphere cooling models. This cooling model may apply well only to ages younger than about 1000 Ma, since the cratons formed under different conditions during the early earth history and appear to have a somewhat different composition (e.g., Griffin et al., 2003). Also, very young lithosphere, less than about 50 Ma, where current brittle deformation is indicated by significant seismicity, may not behave effectively elastically (e.g., Burov and Diament, 1995).

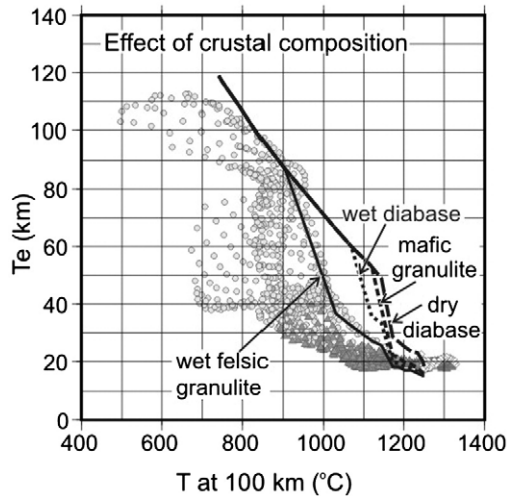


Fig. 10.  $T_e$  versus temperature from Vs compared to Cordillera model relations with Cordillera strain rate of  $10^{-15} \text{ s}^{-1}$ , for varying lower crustal compositions.

Model  $T_e$  as a function of approximate surface heat flow is also shown for this cooling model, assuming that the upper crustal heat generation does not change with time. If upper crust heat generation on average is taken to decrease with age due to the erosion of the high radioactivity uppermost crust (e.g., Hasterok and Chapman, 2007), the heat flow will be slightly lower for each  $T_e$  at the older ages. There is a rapid transition from thin  $T_e$  that includes only the upper crust, to a thick  $T_e$  that includes a significant thickness of upper mantle, at an age of about 300 Ma. At this age the model lithosphere total strength increases quite abruptly with time. The compilation of  $T_e$  versus tectonic age for Europe by Pérez-Gussinyé and Watts (2005) is fit approximately by the predictions of this simple cooling model.

## 8. Discussion and conclusions

There is a clear bimodal division between the North American Cordillera with thin  $T_e$ , slow upper mantle Vs and high inferred upper mantle temperatures, and the adjacent stable platform and Craton with thick  $T_e$ , fast Vs and low inferred temperatures. The corresponding Moho temperatures are about 800–900 °C for the Cordillera and 400–500 °C for the Craton. The sharp lateral step in  $T_e$  reflects an eastward transition from there being significant strength only in the upper crust (little mantle strength) to crust and mantle being strong to a considerable depth. A transition region is expected where there is a weak lower crust with some upper mantle strength (jelly sandwich). The temperature versus depth profiles from Vs data are in general agreement with the temperatures from other sources, including surface heat flow and xenoliths. The exception is that the upper ~30 km of the mantle under the Craton has temperatures inferred from Vs that are too high by 100–200 °C. This discrepancy may result from either an unmodelled phase transition or the mapping of crustal velocities to mantle depths; in either case it warrants further study.

An important feature of the thermal regime in the Cordillera is that temperatures below the base of the lithosphere at about 60 km are approximately adiabatic so that the temperatures at 100 km, and therefore Vs, are decoupled from surface heat flow. Variations in Vs deeper than 60 km therefore may provide useful information on regional composition and state variations in this region. For the Craton where the conductive lithosphere is much thicker, heat flow and inferred deep temperatures are expected and observed to be strongly correlated with Vs at 100 km. In contrast to Vs versus depth,  $T_e$  involves thermally conductive upper 15–30 km of the crust in the Cordillera and conductive 100 km or more lithosphere in the Craton so is strongly correlated with surface heat flow in both regions.

A model effective elastic thickness can be fit to the  $T_e$  and Vs data to a first order using laboratory-derived rheology. Our study supports the conclusion that lithosphere elastic thickness and strength are controlled primarily by temperature, and that laboratory-based rheology provides a good estimate of the deformation behaviour of the crust and upper mantle. For the areas with the highest estimated temperatures from Vs, especially for the Volcanic Arc, the very low velocities may be due to the effect of fluids rather than especially high temperatures. The analysis suggests that mantle strength must contribute substantially to the observed  $T_e$  for the stable Craton region, but must be negligible for the Cordillera and other hot young areas. The upper mantle composition is the primary uncertainty on the strength profiles for the Craton. We are unable to place solid constraints from these data on either the exact composition for each region, but a better fit of the model  $T_e$  to those measured is obtained using for a “wet” Cordillera mantle rheology and a “dry” Craton mantle rheology.

Uncertainties in strain rates give significant uncertainties in model  $T_e$ . To fit the observed  $T_e$  with model  $T_e$ , lower strain rates are required for Craton compared to Cordillera, as expected from other estimates of strain rates. The decoupling stress threshold may be different for the two regions because of the time dependent rheology but we cannot demonstrate the difference from these data. The measured  $T_e$  values have numerous uncertainties and there are a number of questions to be considered in  $T_e$  models; i.e., what are the load durations and the effective strain rates, especially for the Craton compared to the Cordillera, and what is the effect of topographic loads compared to loads from internal crustal density variations. Fortunately 2–3 orders of magnitude change in strain rate are needed to make a significant difference.

Both the measured  $T_e$  and the model  $T_e$  suggest that the weak lower crust with stronger uppermost mantle (jelly sandwich rheology) will occur only for intermediate thermal regimes. Taking our simple cooling model (Currie and Hyndman, 2006), such intermediate temperatures will occur for thermotectonic ages (time after subduction stops) of about 300 Ma, i.e., quite restricted circumstances that are present in only a few areas globally. For younger hotter regions, only the upper 20 km of the crust has significant strength. For older cooler regions, the whole crust and a significant thickness of upper mantle are strong, i.e., to a depth of over 100 km for the Archean cratons.

Our strength estimates support the conclusion that the lithosphere for the Cordillera and other continental backarc mobile belts is weak enough to be deformed by plate boundary forces, whereas the cratons are generally much too strong, i.e., very low inferred strain rates (e.g., Zoback and Townend, 2001). In the Cordillera, the mantle is too hot for brittle failure; earthquakes usually occur only in the cool upper 10–15 km of the crust. In the Craton, earthquakes occur rarely if at all in the upper mantle even though it may be in the brittle regime, probably because the total lithosphere strength is too great for significant deformation under normal plate tectonic forces. In our model the transition from weak to strong lithosphere occurs at a thermotectonic age of about 300 Ma.

## Acknowledgements

We wish to acknowledge the critical  $T_e$  data provided by Paul Flück and Tony Lowry and the assistance with Vs data by Suzan van der Lee. We thank the four reviewers for their very helpful comments that resulted in substantial improvement to the manuscript. Publication No. 20080031 of the Geological Survey of Canada.

## Appendix A. Supplementary data

Supplementary data associated with this article can be found, in the online version, at doi:10.1016/j.epsl.2008.11.023.

## References

- Alfonso, J.C., Ranalli, G., 2004. Crustal and mantle strengths in continental lithosphere: is the jelly sandwich model obsolete? *Tectonophysics* 394, 221–232.
- Audet, P., Mareschal, J.-C., 2004. Variations in elastic thickness in the Canadian Shield. *Earth Planet. Sci. Lett.* 226, 17–31.
- Audet, P., Jellinek, A.M., Uno, H., 2007. Mechanical controls on the deformation of continents at convergent margins. *Earth Planet. Sci. Lett.* 264, 151–166.
- Bürgmann, R., Dresen, G., 2008. Rheology of the lower crust and upper mantle: Evidence from rock mechanics, geodesy and field observations. *Ann. Rev. Earth Plan. Sci.* 36, 531–567. doi:10.1146/annurev.earth.36.031207.124326.
- Burov, E.B., Diament, M., 1995. The effective elastic thickness ( $T_e$ ) of continental lithosphere: what does it really mean? *J. Geophys. Res.* 100, 3 905–3 927.
- Burov, E.B., Watts, A.B., 2006. The long-term strength of continental lithosphere: “jelly sandwich” or “crème brûlée”? *GSA Today* 16, 4–10.
- Cammarano, F., Goes, S., Vacher, P., Giardini, D., 2003. Inferring upper-mantle temperatures from seismic velocities. *Phys. Earth Planet. Inter.* 138, 197–222.
- Clowes, R.M., Zelt, C.A., Amor, J.R., Ellis, R.M., 1995. Lithospheric structure in the southern Canadian Cordillera from a network of seismic refraction lines. *Can. J. Earth Sci.* 32, 1 485–1 513.
- Currie, C., Hyndman, R.D., 2006. The thermal structure of subduction zone backarcs. *J. Geophys. Res.* 111. doi:10.1029/2005JB004024.
- Dixon, J.E., Dixon, T.H., Bell, D.R., Malservisi, R., 2004. Lateral variation in upper mantle viscosity: role of water. *Earth Planet. Sci. Lett.* 222, 451–467.
- Engelbreton, D.C., Cox, A.G., Richard, G., 1984. Relative motions between oceanic plates of the Pacific basin. *J. Geophys. Res.* 89, 10 291–10 310.
- Flück, P., Hyndman, R.D., Lowe, C., 2003. Effective elastic thickness  $T_e$  of the lithosphere in western Canada. *J. Geophys. Res.* 108. doi:10.1029/2002JB002201.
- Forsyth, D.W., 1985. Subsurface loading and estimates of the flexural rigidity of continental lithosphere. *J. Geophys. Res.* 90, 12 623–12 632.
- Frederiksen, A.W., Bostock, M.G., Cassidy, J.F., 2001. S wave velocity structure of the Canadian upper mantle. *Phys. Earth Planet. Inter.* 124, 175–191.
- Gabrielse, H., Yorath, C.J., 1991. The geology of the Cordilleran Orogen in Canada. Geological Survey of Canada, Decade of North American Geology V, G-2.
- Goes, S., van der Lee, S., 2002. Thermal structure of the North American uppermost mantle inferred from seismic tomography. *J. Geophys. Res.* 107. doi:10.1029/2000JB000049.
- Goes, W., Govers, R., Vacher, P., 2000. Shallow mantle temperatures under Europe from P and S wave tomography. *J. Geophys. Res.* 105, 11 153–11 169.
- Griffin, W.L., O'Reilly, S.Y., Abe, N., Aulback, S., Davies, R.M., Pearson, N.J., Doyle, B.J., Kivi, K., 2003. The origin and evolution of Archean lithospheric mantle. *Precambrian Res.* 127, 19–41.
- Griffin, W.L., O'Reilly, S.Y., Doyle, B.J., Pearson, N.J., Coopersmith, H., Kivi, K., Malkovets, V., Pokhilenko, N., 2004. Lithosphere mapping beneath the North American plate. *Lithos* 77, 873–922.
- Hales, A.L., 1969. A seismic discontinuity in the lithosphere. *Earth Planet. Sci. Lett.* 7, 44–46.
- Handy, M.R., 2004. Seismicity, structure and strength of the continental lithosphere. *Earth Planet. Sci. Lett.* 223, 427–441.
- Harder, M., Russell, J.K., 2006. Thermal state of the upper mantle beneath the Northern Cordilleran Volcanic Province, British Columbia, Canada. *Lithos* 87, 1–22.
- Hassani, R., Chéry, J., 1996. Anelasticity explains topography associated with basin and range normal faulting. *Geology* 26, 1095–1098.
- Hasterok, D., Chapman, D.S., 2007. Continental thermal isostasy: 2. Application to North America. *J. Geophys. Res.* 112. doi:10.1029/2006JB004664.
- Hyndman, R.D., Lewis, T.J., 1999. Geophysical consequences of the Cordillera–Craton thermal transition in southwestern Canada. *Tectonophysics* 306, 397–422.
- Hyndman, R.D., Currie, C.A., Mazzotti, S.P., 2005. Subduction zone backarcs, mobile belts, and orogenic heat. *GSA Today* 15, 4–10.
- Jackson, J., 2002. Strength of the continental lithosphere: time to abandon the jelly sandwich? *GSA Today* 16, 4–10.
- Karato, S., 2003. Mapping water content in the upper mantle. Geophysical monograph, vol. 138. Am. Geophys. Un., pp. 135–152.
- Kohlstedt, D.L., Ohlstedt, D.L., Evans, B., Mackwell, S.J., 1995. Strength of the lithosphere: constraints imposed by laboratory experiments. *J. Geophys. Res.* 100, 17 587–17 602.
- Koulakov, I., Sobolev, S.V., Asch, G., 2006. P- and S-velocity images of the lithosphere–asthenosphere system in the Central Andes from local-source tomographic inversion. *Geophys. J. Internat.* 167, 106–126.
- Lebedev, S., Boonen, J., Trampert, J., 2008. Seismic structure of Precambrian lithosphere: New constraints from broad-band surface-wave dispersion. *Lithos* 106. doi:10.1016/j.lithos.2008.06.010.
- Lowry, A.R., Smith, R.B., 1995. Strength and rheology of the western U.S. Cordillera. *J. Geophys. Res.* 100, 17 947–17 963.
- Lowry, A.R., Smith, R.B., 1994. Flexural rigidity of the Basin and Range–Colorado Plateau–Rocky Mountain transition from coherence analysis of gravity and topography. *J. Geophys. Res.* 99, 20,123–20,140.
- Lowry, A.R., Ribe, N.M., Smith, R.B., 2000. Dynamic elevation of the Cordillera, western United States. *J. Geophys. Res.* 105, 23,371–23,390.
- Macario, A., Malinverno, A., Haxby, W.F., 1995. On the robustness of elastic thickness estimates obtained using the coherence method. *J. Geophys. Res.* 100, 15 163–15 172.
- MacKenzie, J.M., Canil, D., 1999. Composition and thermal evolution of cratonic mantle beneath the central Archean Slave Province, NWT, Canada. *Contrib. Mineral. Petrol.* 134, 313–324.
- Mazzotti, S., Adams, J., 2005. Rates and uncertainties on seismic moment and deformation rates in Eastern Canada. *J. Geophys. Res.* 110 (B09301). doi:10.1029/2004JB003510.
- Nakajima, J., Matsuzawa, T., Hasegawa, A., Zhao, D., 2001. Three-dimensional structure of  $V_p$ ,  $V_s$  and  $V_p/V_s$  beneath northeastern Japan: implications for arc magmatism and fluids. *J. Geophys. Res.* 106, 21 843–21 857.
- Pérez-Gussinyé, M., Lowry, A.B., Watts, A.B., 2007. Effective elastic thickness of South America and its implications for intracontinental deformation. *Geochem. Geophys. Geosyst.* 8. doi:10.1029/2006GC001511.
- Pérez-Gussinyé, M., Watts, A.B., 2005. The long-term strength of Europe and its implications for plate-forming processes. *Nature* 436, 381–384.
- Pérez-Gussinyé, M., Lowry, A.R., Watts, A.B., Velicogna, I., 2004. On the recovery of effective elastic thickness using spectral methods: examples from synthetic data and from the Fennoscandian Shield. *J. Geophys. Res.* 109. doi:10.1029/2003JB002788.
- Poudjom Djomani, Y.H., Griffin, W.L., O'Reilly, S.Y., Doyle, B.J., 2005. Lithospheric domains and controls on kimberlite emplacement, Slave Province, Canada: evidence from elastic thickness and upper mantle composition. *Geochem. Geophys. Geosyst.* 6. doi:10.1029/2005GC000978.
- Ranalli, G., 1995. *Rheology of the Earth*, Second ed. Chapman and Hall, London. 413 pp.
- Swain, C.J., Kirby, J.F., 2003. The effect of “noise” on estimates of effective elastic thickness of the continental lithosphere by the coherence method. *Geophys. Res. Lett.* 30. doi:10.1029/2003GL017070.
- Thatcher, W., Pollitz, F.F., 2008. Temporal evolution of continental lithospheric strength in actively deforming regions. *GSA Today* 1–11 (April/May).
- van der Lee, S., Frederiksen, A., 2005. Surface wave tomography applied to the North American upper mantle. In: Levander, A., Nolet, G. (Eds.), *Seismic data analysis and imaging with global and local arrays*. Geophys. Monogr., vol. 157. Am. Geophys. Union, Washington, D.C., pp. 67–80.
- van der Lee, S., Nolet, G., 1997. Upper-mantle S-velocity structure of North America. *J. Geophys. Res.* 102, 22 815–22 838.
- Wang, Y., Mareschal, J.-C., 1999. Elastic thickness of the lithosphere in the Central Canadian Shield. *Geophys. Res. Lett.* 26, 3 033–3 035.
- Watts, A.B., 1992. The effective elastic thickness of the lithosphere and the evolution of foreland basins. *Basin Res.* 4, 169–178.
- Watts, A.B., 2007. “An overview”, crust and lithosphere dynamics (Ed. A.B. Watts). In: Schubert, G. (Ed.), *Treatise on Geophysics*, vol. 6. Elsevier, pp. 1–49.
- Watts, A.B., Burov, E.B., 2003. Lithospheric strength and its relationship to the elastic and seismogenic layer thickness. *Earth Planet. Sci. Lett.* 213, 113–131.
- Wiens, D.A., Smith, G.P., 2003. Seismological constraints on structure and flow patterns within the mantle wedge. In: Eiler, J. (Ed.), *Inside the Subduction Factory*. Geophys. Monogr., vol. 138. Am. Geophys. Un., Washington, D.C., pp. 59–81.
- Zoback, M.D., Townend, J., 2001. Implications of hydrostatic pore pressures and high crustal strength for the deformation of intraplate lithosphere. *Tectonophysics* 336, 19–30.
- Zoback, M.D., Townend, J., Grollimund, B., 2002. Steady-state failure equilibrium and deformation of intraplate lithosphere. *Geol. Rev.* 44, 383–401.